Available online at www.sciencedirect.com
ScienceDirect
Polymer 48 (2007) 894–900
polymer
www.elsevier.com/locate/polymer

Experimental and theoretical characterization of the morphologies in fluorinated polyurethanes

Li-Fen Wang*

Department of Applied Chemistry, Fooyin University, 151 Chin-Hsueh Road, Ta-Liao Hsiang, Kaohsiung, Hsien 831, Taiwan, ROC

Received 25 September 2006; received in revised form 27 November 2006; accepted 28 November 2006
Available online 22 December 2006

Abstract

On the analyses of modulated differential scanning calorimetry, Fourier transform infrared spectra and quantum chemical calculations of fluorinated and corresponding unfluorinated polyurethanes, we investigated the effects of fluorination on the intermolecular hydrogen bonds and resulted morphological changes in polyurethanes. The B3LYP/6-31G(d′,p′) calculated values supported the experimental results suggesting that the fluorinated hard segment facilitates hydrogen bond interactions towards soft segment polyether, while reducing the strengths within self-associated hard segments.

Keywords: Fluorinated polyurethane; Hydrogen bonding; Quantum chemical calculation

1. Introduction

Fluorinated polyurethanes (FPUs) with low surface energy have attracted considerable interest in the field of cardiovascular prostheses. Prostheses treated with a fluorinated film deposition offered a dramatic improvement in resistance to the formation of thrombi and emboli [1–9]. Also, incorporation of fluorine into polyurethanes (PUs) changed the morphology of PUs that plays an important role in the biocompatibility of PUs [3,10–17]. To further clarify the effects of surface energy and morphological changes, it is important to elucidate the fluorination effects on the structure and conformational properties of FPU. Typically, PUs exhibit a microphase-separated structure by an association or aggregation of urethane units. The urethane units formed a separate phase (hard segment domain) and acted as a physical cross-link between soft segment domains. The association of urethane segments is accompanied with the formation of diverse hydrogen bonds in which the proton donor and acceptor are the N–H group of the urethane linkage and the oxygen atoms of both polyether and urethane carbonyl, respectively [10,11]. The structure of such a physical network lends itself to quite effective control by the strength of the hydrogen bonds [18].

Differential scanning calorimetry (DSC) providing the glass transition temperature (T_g), melting temperature (T_m) and heat of fusion (ΔH_m) has been widely used to study the hydrogen bonds and microphase-separated structures for PUs experimentally [3,18–28]. The measured T_g of soft segment gave an estimate in the extent of phase mixing about the hard segment dissolving in the soft segment domains. An increase in the percentage of hard segments dissolving in the soft segment domains gave a rise in T_g. For T_m and ΔH_m, the two properties gave an insight into the strength of hydrogen bond in microcrystalline hard segment domains. As the hydrogen bonding gets stronger, T_m and ΔH_m show systematic increases [27]. Also infrared (IR) analysis revealing the absorption bands of carbonyl group (C=O) vibrations provided a further understanding in the type, extent and strength of competitive hydrogen bonding in PUs.

Due to a big advance in computer architecture and algorithms of computational chemistry recently, molecular modeling has provided a powerful and reliable tool to explore the

* Tel.: +886 7 7811151x613; fax: +886 7 7826732.
E-mail address: sc112@mail.fy.edu.tw

0032-3861/$ - see front matter © 2006 Elsevier Ltd. All rights reserved.
doi:10.1016/j.polymer.2006.11.063

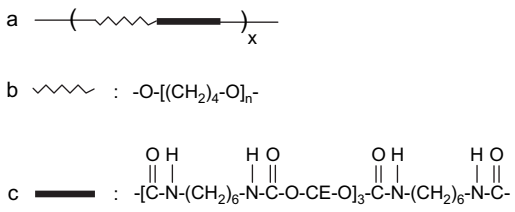

Fig. 1. Schematic structure of studied polyurethanes: (a) polymer; (b) soft segment; (c) hard segment. Group CE (chain extender) in hard segment represents $-CH_2(CF_2)_2CH_2-$ and $-(CH_2)_4-$ for FB- and BD-polymer, respectively.

hydrogen bond strengths and vibration spectra of molecules or molecular complexes [25,29–35]. For example, Yang et al. [32,33] carried out molecular mechanics (MM) calculations with COMPASS force field to investigate different types of hydrogen bond interaction and energies in PUs. They recommended that the self-associated urethane groups were the predominant hydrogen bond complexes for the interaction within the hard segments, whereas the probability of urethane N–H forming the hydrogen bond with the urethane alkoxy oxygen appeared low. Also, Yilgör et al. [31] calculated the hydrogen bond energies and lengths of the urea, urethane and ether model compound complexes by B3LYP [36] and MP2 [37] methods. They expected that appreciable amount of phase mixing between hard and soft segments in PUs existed. However, to our knowledge, there are few applications of quantum chemical calculations in studying the fluorine-containing PUs.

To better understand the hydrogen bond interactions in FPUs, a fluorinated polyurethane, FB-polymer with chain extender $-CH_2(CF_2)_2CH_2-$ having high content of hard segment (64.1 wt%) was synthesized in this work. Also, unfluorinated polyurethane (designated as BD-polymer) chain extended with extender $-(CH_2)_4-$ was prepared in same stoichiometry for a comparison (Fig. 1). Modulated DSC (MDSC) [38–42], Fourier transform infrared (FTIR) analysis and complementary quantum chemical calculations were performed to characterize the effects of fluorinated hard segment on the intermolecular hydrogen bonds and morphologies in PUs.

2. Methods

2.1. Materials

Hydroxyl-terminated poly(tetramethyl oxide) with molecular weights of 650 g/mol (PTMO; Aldrich) was dehydrated under vacuum at 60 °C for 48 h before use. Hexamethylene diisocyanate (HDI; Aldrich), stannous octoate (T-9; Sigma), and 2,2,3,3-tetrafluoro-1,4-butanediol (FB; Lancaster) were used as obtained. 1,4-Butanediol (BD; Tedia) and dimethylacetamide (DMAc; Tedia) were distilled under vacuum from calcium hydride and then dried over 4 Å molecular sieves before use.

2.2. Preparation and characterization of fluorinated polyurethanes

The fluorinated and unfluorinated polyurethanes, designated as FB- and BD-polymer, respectively, were synthesized using HDI, PTMO and chain extender in a 4:1:3 stoichiometry. The predetermined amount of HDI was dissolved in DMAc in a four-necked flask under nitrogen and a fixed amount of PTMO/DMAc solution containing 0.5 wt% stannous octoate as the catalyst was added dropwise at 60 °C. After addition of the PTMO solution, the temperature was raised to 70 °C and kept for 1 h. In a second step, the stoichiometric amount of chain extender was added drop by drop and the reaction was carried out at 90 °C. Reaction completion was monitored by the absence of IR-absorption of the free NCO group at 2270 cm^{-1}. Polyurethanes obtained were precipitated in deionized water, washed thoroughly with methanol, and dried in a vacuum oven at 60 °C for 1 week [43].

FTIR absorption spectrum of FB-polymer has a 1180 cm^{-1} band resulting from CF_2 stretch [44], which is not observed in the IR spectrum of BD-polymer. This indicated the presence of fluorocarbon segments in FB-polymer. Elemental analysis revealed the element compositions (wt%) of synthesized polymers being in agreement with those predicted from stoichiometric values:

FB-polymer: C: 52.20, H: 7.59, N: 6.14 (stoichiometric C: 52.51, H: 7.65, N: 6.19).

BD-polymer: C: 59.44, H: 9.43, N: 7.99 (stoichiometric C: 59.63, H: 9.44, N: 7.03).

From the gel permeation chromatography data, the yielded FB-polymer had number- and weight-averaged molecular weight of 3.2×10^4 and 5.0×10^4 g/mol, respectively, and BD-polymer had 7.3×10^4 and 11.2×10^4 g/mol, respectively.

As film specimens, we investigated both of the PU samples in the main IR spectral region by using the Bio-Rad FTS-40A Fourier transform infrared spectrophotometer operated with a dry air purge. Sixty-four scans at 2 cm^{-1} resolution were signal averaged. The films were cast from 1 wt% solution of PUs in dimethylacetamide (DMAc; Tedia) on KBr plates. We removed the solvent by putting the sample in an oven at 60 °C and finally under vacuum.

MDSC experiments (TA Instruments 2920 DSC, equipped with a liquid nitrogen cooling accessory) utilized heating ramps of 5 °C/min, and modulated amplitude of 0.796 °C with a period of 60 s [41,42]. A second scan from −120 to 200 °C was recorded.

2.3. Quantum chemical calculations

We used the Gaussian 03 program [45] to carry out B3LYP/6-31G(d′,p′) calculations on the urethane model compounds and complexes. Computation of the interaction energy between various hydrogen (proton) donor–acceptor pairs went through a supermolecular approach where the ground state energy of the hydrogen-bonded complex was calculated and compared to the sum of the ground state energies of the individual components.

Table 1 gives the chemical structures of the model compounds used in this study. We used 1,4-di-(3′-propylcarbamate)butane (U), 2,2,3,3-tetrafluoro-1,4-di-(3′-propylcarbamate)butane (T) and diethylether (E) to model the unfluorinated urethane, fluorinated urethane and soft segment polyether,

Table 1
The chemical structures of the model compounds considered in quantum chemical calculations

Segment	Chemical structure	Code
Polyether	Diethylether (CH_3CH_2–O–CH_2CH_3)	E
Urethane	1,4-Di-(3′-propylcarbamate)butane ($CH_3CH_2CH_2$–NHCOO–$(CH_2)_4$OOCNH–$CH_2CH_2CH_3$)	U
Fluorinated urethane	2,2,3,3-Tetrafluoro-1,4-di-(3′-propylcarbamate)butane ($CH_3CH_2CH_2$–NHCOO–$CH_2(CF_2)_2CH_2$OOCNH–$CH_2CH_2CH_3$)	T

respectively. The urethane model compound consists of a repeat unit of hard segment, i.e., one HDI and one chain extender (FB or BD). There are two urethane groups in the model compounds. We adopted urethane–ether, urethane dimer and urethane trimer shown in Fig. 2 to model the hard–soft segment interaction, the hard segment associates in loosely ordered hard segment domain, and the hard segment associates in ordered (microcrystalline) hard segment domain, respectively [24].

According to the wide-angle X-ray diffraction results [46–50], the chain conformation of hard segment is highly extended in the microcrystalline region. The hard segment rods pack in parallel and arrange in an orderly manner with the ordered urethane hydrogen bonds being of the planar form. The proton donor and acceptor of the hydrogen bonds are the N–H group and carbonyl oxygen of the urethane linkage. Thus, in this work self-associated urethane groups were considered the predominant hydrogen bonds for the interaction within the hard segment.

Starting from the Austin Model 1 (AM1) [51] optimized geometries of model compounds and their complexes, B3LYP/6-31G(d′,p′) calculations were carried out to do further geometry optimizations and frequency calculations. The dagger basis set, (d′,p′), utilized the exponents from the d and p functions in the 6-311G basis set attempts to remedy some deficiencies in the standard of 6-31G(d,p) basis set, which is necessary for modeling fluorine-containing compounds. Atomic charge distributions were performed by Mulliken population analysis at B3LYP/6-31G(d′,p′) level.

3. Results and discussion

3.1. Experimental

Table 2 gives the experimental MDSC and FTIR data for BD- and FB-polymer. Every polymer gave two thermal transitions indicating T_g of soft segment domains and T_m of microcrystalline hard segment domains, respectively. The FB-polymer has a higher T_g (230 K) but lower T_m and ΔH_m (413 K and 113 J/g, respectively) compared with the BD-polymer ($T_g = 224$ K, $T_m = 430$ K and $\Delta H_m = 167$ J/g). The pure soft segment PTMO gave a value of 188 K for T_g [43]. Both of the polymers exhibited a rise in T_g, ΔT_g is 36 K and 42 K for BD- and FB-polymer, respectively. This resulted from a substantial percentage of hard segments dissolving in the soft segment domains for both polymers. Also, the FB-polymer had a high value of T_g than BD-polymer. The higher value of ΔT_g in FB-polymer compared to BD-polymer was attributed to both the fluorinated hard segments favoring their

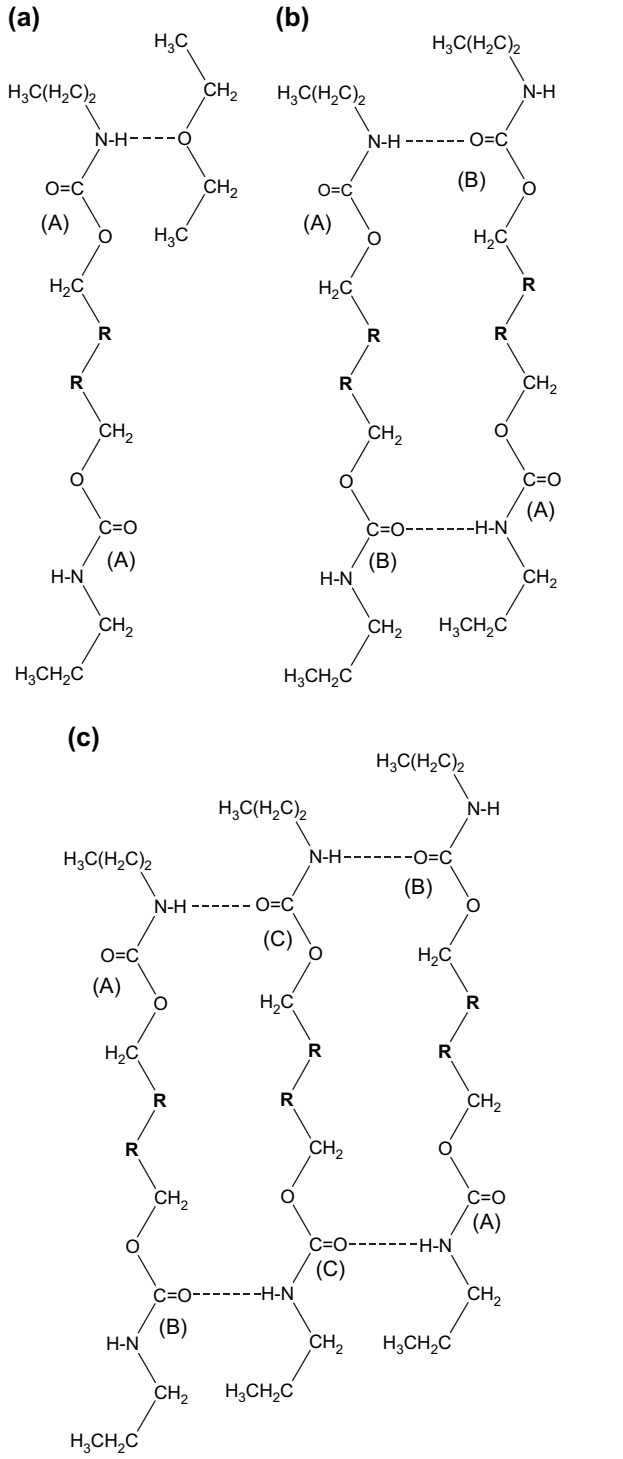

Fig. 2. Three complexes in model system: (a) urethane–ether, (b) urethane dimer and (c) urethane trimer. Group R denotes $-CF_2-$ and $-CH_2-$ for fluorinated (T) and unfluorinated (U) urethane, respectively. The hydrogen bonding in these complexes is indicated by a dotted line.

Table 2
Experimental MDSC and FTIR analyses

Material	T_g (K)	ΔT_g [a] (K)	T_m (K)	ΔH_m [b] (J/g)	$\nu_{C=O}$ (cm^{-1})
BD-polymer	224	36	430	167	1722, 1708, 1685
FB-polymer	230	42	413	113	1742, 1722, 1704

[a] $\Delta T_g = T_g - T_{g,PTMO}$, where $T_{g,PTMO}$ is the glass transition temperature of pure PTMO.
[b] Calculated based on 1 g of hard segments.

solubility in soft segment domain and the steric hindrance of bulkier fluorine atom than H atom that increases the energy required to rotate the soft segment. For the values of T_m and ΔH_m, the FB-polymer exhibited lower values of T_m and ΔH_m compared to BD-polymer. This indicated that the fluorination of hard segment hinders the microcrystalline ordered arrangement and reduces the intermolecular hydrogen bonds in hard segment domains.

IR spectra gave multiple C=O absorption bands comprising three major components at 1722, 1708, 1685 cm^{-1} for BD-polymer and 1742, 1722, 1704 cm^{-1} for FB-polymer (Table 2). The first band (1722 and 1742 cm^{-1} for BD- and FB-polymer, respectively) resulted from the carbonyls without hydrogen bonding, and the other components are generally associated with urethane groups included in the hydrogen bonds with various energies [3,24–26,52]. All C=O absorption components in FB-polymer were noted to blue shift relative to BD-polymer [3,52]. It was related to both the inductive and mesomeric effects contributed from the fluorine-containing group attached to the carbonyl group. Mesomeric effect leads to the existence of polar contributing form $X^+{=}C(R){-}O^-$ with C–O in single bond, suppressing X–C(R)=O form with C=O in double bond. Thus, this effect decreases the double bond character of C=O. Inductive effect reduces the length of the carbonyl bond and thus increases its double bond character. Introduction of electron withdrawing groups of fluorine enhances the inductive effect and decreases simultaneously the mesomeric effect, thus increasing C=O force constant and consequently the frequency of absorption.

3.2. Quantum chemical calculations

Calculated hydrogen bond energies and frequencies of C=O stretch by using B3LYP/6-31G(d′,p′) calculations are listed in Table 3, where the optimal geometries of hydrogen-bonded U–U–U and T–T–T trimers are shown in Fig. 3. The U associates, U–U and U–U–U for dimer and trimer, respectively, had a larger hydrogen bond energies of 60.4 and 61.6 kJ/mol for dimer and trimer, respectively, than the T associates, T–T and T–T–T for dimer (54.6 kJ/mol) and trimer (58.2 kJ/mol), respectively. This is in agreement with experimental data that BD-polymer has a higher T_m and ΔH_m than FB-polymer. The reduction in the strength of hydrogen bond in fluorinated urethane (T) associates is attributed to both the steric and inductive effects induced by fluorination. As shown in Fig. 3, the introduction of fluorine leads to a significant change of the dihedral angle of $-C(F_2)-C-O-C(O)-$ from 180° in urethane U to 110° in T. Thus, the presence of

Table 3
Hydrogen bond energies (E_{HB}) and vibration frequencies of C=O stretchings ($\nu_{C=O}$) by the B3LYP/6-31G(d′,p′) calculations

Molecule or complex	E_{HB} [a] (kJ/mol)	$\nu_{C=O}$ (cm^{-1})		
		(A)	(B)	(C)
U	–	1814	–	–
U–E	22.9	1808	–	–
U–U	60.4	1808	1783	–
U–U–U	61.6	1807	1785	1768
T	–	1830	–	–
T–E	33.4	1822	–	–
T–T	54.6	1827	1802	–
T–T–T	58.2	1826	1802	1785

[a] Calculated hydrogen bond energy between two monomers.

fluorine gives rise to steric hindrance that causes the bend of chain and makes close packing of polymer chains more difficult. Also, an analysis of charge distributions by Mulliken population gave the partial atomic charges of carbonyl oxygen, −0.420, and carbonyl carbon, 0.574, for fluorinated urethane (T) and −0.437 and 0.581 for unfluorinated urethane (U). Fluorination leading to a reduction in electron density of carbonyl oxygen acts as another factor hindering the hydrogen bond interactions of urethane associates.

Additionally, owing to the strong electronegativity of the fluorine, the hydrogen bond energy between fluorine on C–F of the chain extender and proton on the N–H of the urethane groups was calculated. The hydrogen bond energy obtained was 43.0 kJ/mol, which is 11.6 kJ/mol lower than the self-urethane interaction. Thus, this significant interaction between C–F and N–H groups may also exist in FPUs, contributed to hinder the ordered arrangement of hard segments.

Hydrogen bond energies of competitive urethane–ether (U–E and T–E) type hydrogen bonding were computed to be 22.9 and 33.4 kJ/mol, respectively, which are smaller than the values of 60.4 and 54.6 kJ/mol for urethane associates U–U and T–T, respectively. This recommended a substantial phase mixing due to hydrogen bonding that appeared in mixture of hard segment urethane and soft segment ether (or in polyether based polyurethanes) [31] and was also consistent with MDSC results, in which both of the studied PUs had a significant raise in soft segment T_g. Also, a higher E_{HB} in T–E type hydrogen bonding, 33.4 kJ/mol, compared with U–E type, 22.9 kJ/mol, reflects that fluorinating hard segment of PUs promotes increased phase mixing and elevation of T_g.

Table 3 also lists the calculated C=O vibrational frequencies ($\nu_{C=O}$). Carbonyl (A) represents the C=O without hydrogen bonding (Fig. 2). As observed in this table, when hydrogen bonding of urethane occurs to an ether group via N–H group (U–E and T–E), the neighboring C=O vibration absorbs at nearly the same frequency (1808 and 1822 cm^{-1} for complexes *U*–E and *T*–E) as that when a bridge to a carbonyl group is formed (1808 and 1827 cm^{-1} for complexes *U*–U and *T*–T). These calculated frequencies slightly differ from that of isolated carbonyls and agree with the experimental results found in the literature [24].

Hydrogen-bonded carbonyl (B) (neighboring N–H remains free) in dimers and trimers shifts its vibration to lower

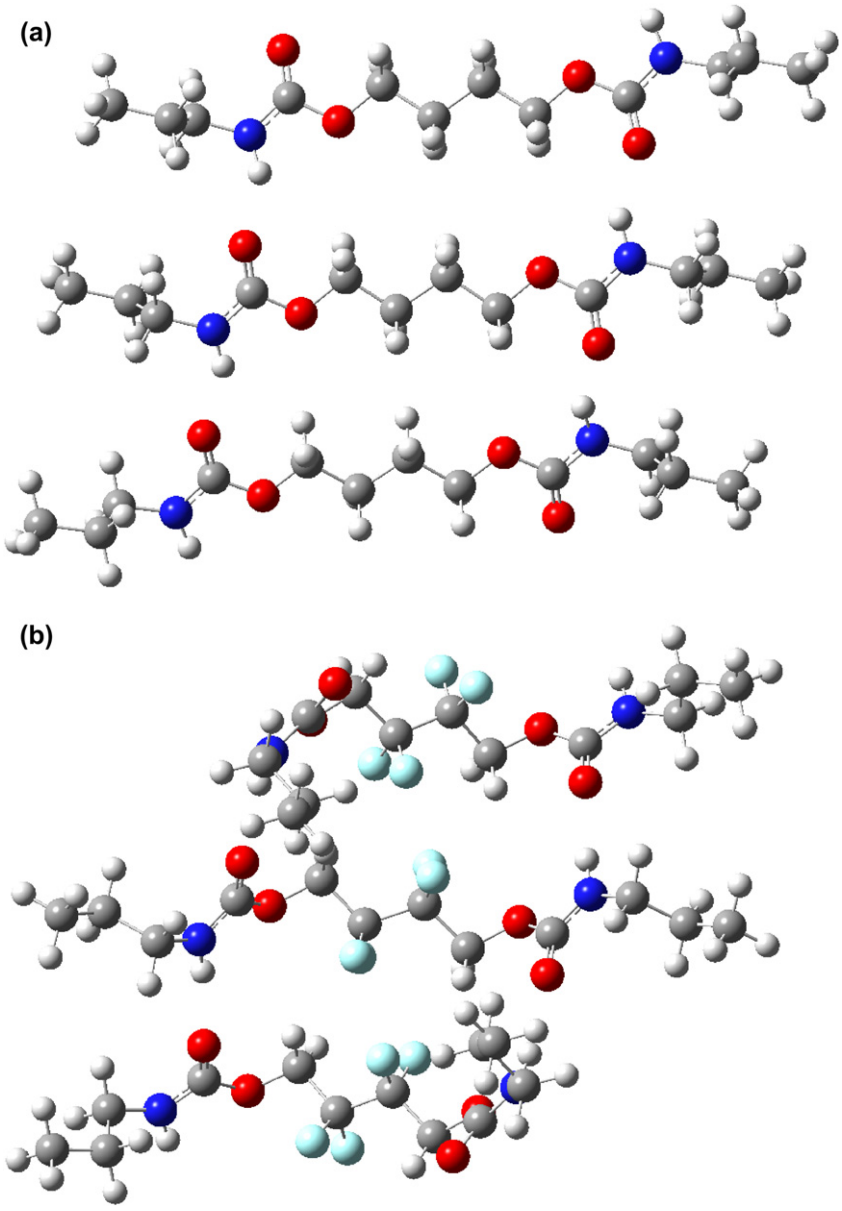

Fig. 3. Optimal geometries of hydrogen-bonded (a) U–U–U and (b) T–T–T trimers.

frequency (e.g., 1783 and 1802 cm^{-1} for complexes U–*U* and T–*T*) with a change of 22–25 cm^{-1} compared with the carbonyl (A). The lowest frequency (i.e., 1768 cm^{-1} for complex U–U–U and 1785 cm^{-1} for complex T–T–T) shifted from carbonyl (A) by ca. 40 cm^{-1} is associated with the carbonyl group (C) of urethane included in the most ordered hydrogen bond moieties (both of the N–H and C=O groups are hydrogen bonded with adjacent urethane), i.e., those situated inside associate of urethane groups. Fig. 4 shows the relationships between experimental and calculated frequencies of C=O stretching for complexes U–U–U and T–T–T, a linear relationship was obtained with a slope of 0.9545 and a *R*-square larger than 0.98. As shown in Fig. 5, the scaled FTIR spectra obtained for U–U–U and T–T–T from quantum chemical calculations were consistent with the experimental spectra of BD- and FB-polymer.

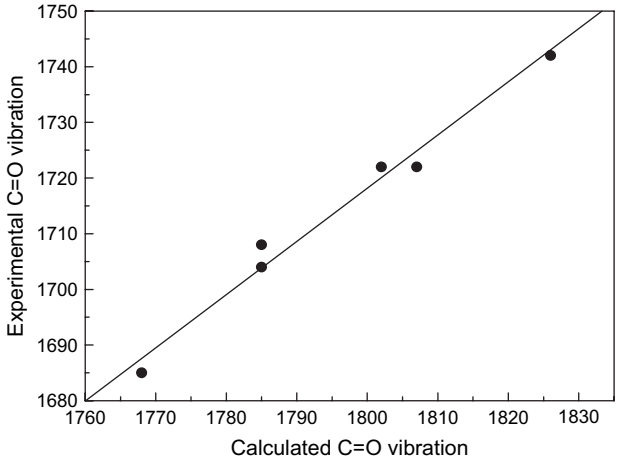

Fig. 4. Relationships between calculated and experimental frequencies (in cm^{-1}) of C=O stretching for U–U–U and T–T–T trimers.

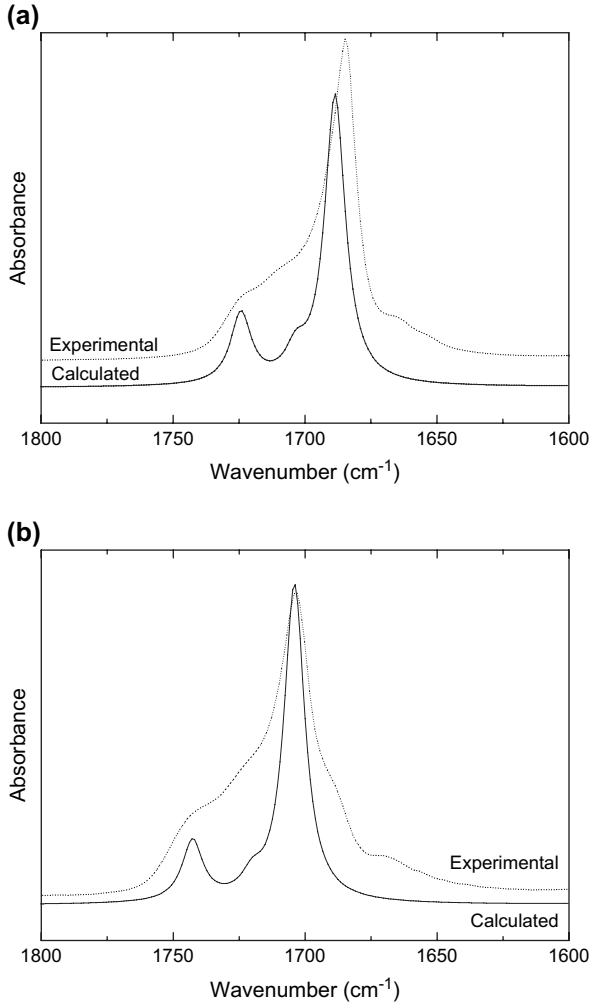

Fig. 5. Calculated (—) and experimentally obtained (- - -) C=O stretching region of FTIR spectra for (a) model U–U–U trimer and BD-polymer; (b) model T–T–T trimer and FB-polymer.

4. Summary

Using the model compounds of diethylether (E), 1,4-di-(3′-propylcarbamate)butane (U) and 2,2,3,3-tetrafluoro-1,4-di-(3′-propylcarbamate)butane (T) to model soft segment polyether, unfluorinated urethanes and fluorinated urethanes, the B3LYP/6-31G(d′,p′) calculations provided quantitative information on hydrogen bonds supporting experimental MDSC and FTIR results. With ether–urethane type hydrogen bond, fluorinated urethane has more hydrogen bond energy by ca. 10 kJ/mol than unfluorinated urethane. This yields extensive phase mixing between hard and soft segments and reduces the urethane associates type hydrogen bonding. Also, steric hindrance and inductive effects of fluorine also exert important influences on hindering the hydrogen bonding of urethane associates. These results illustrate the observation in MDSC that fluorination of PU leads to an elevation (ca. 6 K) of glass transition temperature and a reduction (ca. 17 K) of melting temperature. Finally, scaled by a factor of 0.9545, the calculated vibrational frequencies of carbonyls from B3LYP/6-31G(d′,p′) method are in agreement with experimental FTIR spectra.

Acknowledgements

The author thanks the simulation laboratory of Fooyin University for a large allotment of computation resources and technical support.

References

[1] Massa TM, Yang ML, Ho JYC, Brash JL, Santerre JP. Biomaterials 2005;26:7367.
[2] Tan H, Xie X, Li J, Zhong Y, Fu Q. Polymer 2004;45:1495.
[3] Tan H, Guo M, Du R, Xie X, Li J, Zhong Y, et al. Polymer 2004;45:1647.
[4] Hawkridge AM, Gardella Jr JA, Toselli M. Macromolecules 2002;35:6533.
[5] Cohn D, Stern T. Macromolecules 2000;33:137.
[6] Yang M, Santerre J. Biomacromolecules 2001;2:134.
[7] Kwok CS, Mourad PD, Crum LA, Ratner BD. Biomacromolecules 2000;1:139.
[8] Guerra RSD, Lelli L, Tonelli C, Trombetta T, Cascone MG, Taveri M, et al. J Mater Sci Mater Med 1994;5:452.
[9] Pizzoferrato A, Arciola CR, Cenni E, Ciapetti G, Sassi S. Biomaterials 1995;16:361.
[10] Kim YS, Lee JS, Ji Q, McGrath JE. Polymer 2002;43:7161.
[11] McCloskey CB, Yip CM, Santerre JP. Macromolecules 2002;35:924.
[12] Tonelli C, Ajroldi G, Turturro A, Marigo A. Polymer 2001;42:5589.
[13] Grasel TG, Cooper SL. Biomaterials 1986;7:315.
[14] Hsu SH, Lin ZC. Colloids Surf B Biointerfaces 2004;36:1.
[15] Huang SL, Chao MS, Ruaan RC, Lai JY. Eur Polym J 2000;36:285.
[16] Tonelli C, Ajroldi G, Marigo A, Marego C, Turturro A. Polymer 2001;42:9705.
[17] Tan H, Li J, Guo M, Du R, Xie X, Zhong Y, et al. Polymer 2005;6:230.
[18] Zharkov VV, Strikovsky AG, Verteletskara TE. Polymer 1993;34:938.
[19] Versteegen RM, Kleppinger R, Sijbesma RP, Meijer EW. Macromolecules 2006;39:772.
[20] Kojio K, Fukumaru T, Furukawa M. Macromolecules 2004;37:3287.
[21] Queiroz DP, de Pinho MN. Polymer 2005;46:2346.
[22] Wilhelm C, Gardette JL. Polymer 1997;38:4019.
[23] Luo N, Wang DN, Ying SK. Macromolecules 1997;30:4405.
[24] Marcos-Fernández A, Lozano AE, González L, Rodríguez A. Macromolecules 1997;30:3584.
[25] Wang SK, Sung CSP. Macromolecules 2002;35:877.
[26] Yen FS, Hong JL. Macromolecules 1997;30:7927.
[27] Yilgör E, Burgaz E, Yurtsever E, Yilgör İ. Polymer 2000;41:849.
[28] Hesketh TR, van Bogart JWC, Cooper SL. Polym Eng Sci 1980;20:190.
[29] van der Wijst T, Guerra CF, Swart M, Bickelhaupt FM. Chem Phys Lett 2006;426:415.
[30] Smith GD, Bedrov D, Byutner O, Borodin O, Ayyagari C. J Phys Chem A 2003;107:7552.
[31] Yilgör E, Yilgör İ, Yurtsever E. Polymer 2002;43:6551.
[32] Ren Z, Zeng X, Yang X, Ma D, Hsu SL. Polymer 2005;46:12337.
[33] Ren Z, Ma D, Yang X. Polymer 2003;44:6419.
[34] Bandekar J, Okuzumi Y. J Mol Struct (Theochem) 1993;281:113.
[35] Genovese A, Shanks RA. Comput Theor Polym Sci 2001;11:57.
[36] Becke AD. J Chem Phys 1993;98:5648.
[37] Møller C, Plesset MS. Phys Rev 1934;46:618.
[38] Di Lorenzo ML, Wunderlich B. Thermochim Acta 2003;405:255.
[39] Okazaki I, Wunderlich B. Macromolecules 1997;30:1758.
[40] Wunderlich B. Prog Polym Sci 2003;28:383.
[41] Sauer BB, Kampert WG, Blanchard EN, Threefoot SA, Hsiao BS. Polymer 2000;41:1099.
[42] Kampert WG, Sauer BB. Polymer 2001;42:8703.
[43] Wang LF. Eur Polym J 2005;41:293.
[44] Mohan J. Organic spectroscopy: principles and applications. New Delhi: Narosa; 2001.

[45] Frisch MJ, Trucks GW, Schlegel HB, Scuseria GE, Robb MA, Cheeseman JR, et al. Gaussian 03, revision C.02. Wallingford CT: Gaussian Inc; 2004.
[46] McKiernan RL, Sikorski P, Atkins EDT, Gido SP, Penelle J. Macromolecules 2002;35:8433.
[47] Blackwell J, Nagarajan MR. Polymer 1981;22:202.
[48] Bonart R, Morbitzer L, Hentze G. J Macromol Sci Phys 1969;B3:337.
[49] Bonart R, Morbitzer L, Müller EH. J Macromol Sci Phys 1974;B9:447.
[50] Wilkes CE, Yusek CS. J Macromol Sci Phys 1973;B7:157.
[51] Dewar MJS, Zoebisch EG, Healy EF, Stewart JJP. J Am Chem Soc 1985;107:3902.
[52] Yoon SC, Ratner BD. Macromolecules 1988;21:2392.